PHYSICAL REVIEW C VOLUME 20, NUMBER 5 NOVEMBER 1979

Realistic effective interactions for the *sd* shell: Global and discrete nuclear properties

B. J. Dalton, W. J. Baldridge,* and J. P. Vary
Ames Laboratory, United States Department of Energy and Physics Department, Iowa State University, Ames, Iowa 50011
(Received 30 January 1979)

Comparisons of the Kuo and Vary-Yang *sd* shell realistic effective shell-model interactions are presented through studies of the resulting global and discrete nuclear properties. The methods of spectral distributions are used to obtain energy moments for ^{21}Ne and spin cutoff factors for ^{28}Si for each interaction. Shell-model spectra are presented for some mass $A = 18$ to $A = 21$ *sd* shell nuclei. In each case we show for comparison the results using the Chung-Wildenthal empirical interaction. In addition to demonstrating the role of various approximations through resulting global and discrete properties, we show that certain conclusions drawn from global properties are consistent with those based upon discrete properties.

[NUCLEAR STRUCTURE Realistic effective interactions for *sd* shell, spectral distribution theory, level densities, and spin cutoff factors.]

I. INTRODUCTION

In the construction, via Brueckner theory,[1,2] of a realistic effective nuclear Hamiltonian, practical considerations require truncation of the expansion at low order in the G matrix as well as other approximations. There is much current interest in the effects of such approximations on calculated properties of nuclei.[2,3]

In the present study we compare energy moments, spin cutoff factors, and shell-model spectra calculated with the Kuo[4] and Vary-Yang[5] (VY) *sd* shell effective interactions.

We also make calculations with the Chung-Wildenthal[6] (CW) empirical interaction. The VY interaction is given as a function of a gap parameter (labeled C) which shifts the energies of the particle orbits with respect to valence and core states. We show that a choice of $C \simeq 20$ MeV minimizes a χ^2 measure of the deviation between the VY and CW interactions and discuss the significance of this gap. We also add to the VY interaction higher partial wave contributions which we obtain via the Sussex[7] method. In addition we study the contribution of a single important third order diagram.[8] The effects on the shell-model spectra resulting from these corrections are discussed.

In Sec. II we discuss some of the approximations used in obtaining the Kuo and VY interactions. We also describe the above mentioned χ^2 determination of an optimal gap parameter and compare the results with other related studies.

We review briefly in Sec. III the spectral distribution methods[9] used to calculate level densities, binding energies,[10] and spin cutoff factors.[11] In this section we calculate the level density for ^{21}Ne with spectral distribution techniques for $J = \frac{9}{2}$ and compare with the histogram obtained from exact diagonalizations. Using these moment techniques we calculate for ^{21}Ne the energy centroid and width for each spin and interaction mentioned above. Using a refinement of the spectral distribution approach which expands in terms of configurations we calculate the spin cutoff factor for ^{28}Si and compare the results deduced from the ^{25}Mg(α, n)-^{28}Si reaction at different energies.[11]

We conclude in Sec. IV with comparisons of the shell-model spectra calculated using the Rochester–Oak Ridge Shell Model Code.[12]

II. NUCLEAR HAMILTONIANS

Both the Kuo[4] and Vary-Yang[5] (VY) realistic effective interactions for the *sd* shell, with an ^{16}O core, have been derived from potentials which fit nucleon-nucleon scattering data and deuterium properties. The method employed is the Bloch-Horowitz-Brandow[13] formulation of the realistic nuclear shell-model problem. For the *sd* valence space, both of the above mentioned effective interactions $V_{\rm eff} = H_{\rm eff} - H_0$ are obtained by evaluating the linked diagrams of

$$V_{\rm eff} = G + GQ'(E_0 - H_0)^{-1} V_{\rm eff} \tag{2.1}$$

through second order in the Brueckner reaction matrix G. Here Q' projects onto states outside the model space but not included in G. In particular, Q' projects onto some particle-hole (p-h) states. The bare interaction G is itself the solution of

$$G = V + VQ(E_0 - H_0)^{-1} G\,, \tag{2.2}$$

where Q is the Pauli operator and projects onto unoccupied two-particle states.

Although both the Kuo and VY interactions were obtained by solving (2.1) through second order in G, these two interactions differ in a number of

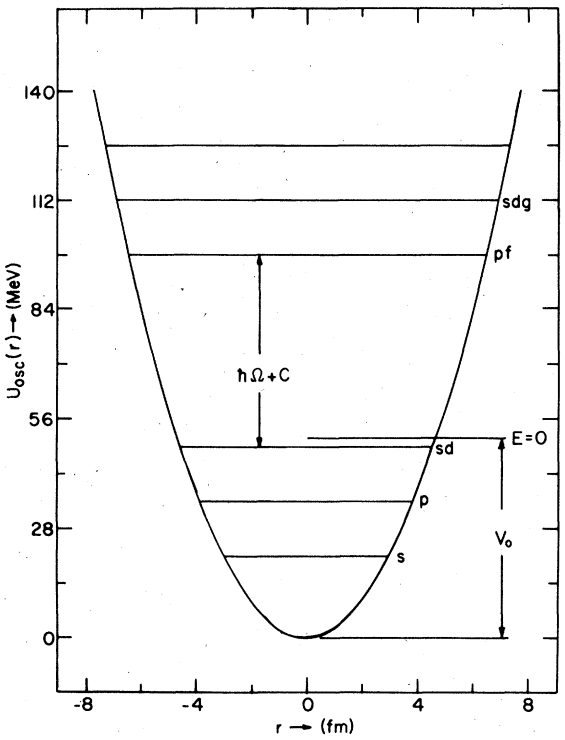

FIG. 1. Spectrum of the shifted oscillator potential. C is the energy of the shift between the valence model space and the remaining unoccupied states. The constant V_0 is chosen to put the oscillator *sd* shell at the centroid of experimental *sd* shell states to define H_0 for the calculation of G.

important ways, including the potential V that was chosen. In spite of this and some other differences discussed below, the on-shell bare G matrices are approximately equal for a range of C values between 15 and 30 MeV. The Kuo effective interaction is based on the Hamada-Johnston[14] potential and has the severe approximation that the summation on the intermediate p-h states in the important core-polarization term was truncated at $2\hbar\Omega$ (or about 30 MeV) excitation. The VY effective interaction[5] is based on the Reid soft core potential[15] and is given as a function of the energy gap C. In H_0, VY take the lowest-lying oscillator unoccupied orbits (the *pf* shell) to lie $\hbar\Omega + C$ above the valence orbitals (the *sd* shell) as illustrated in Fig. 1. All other major-shell spacings are taken to be $\hbar\Omega = 14$ MeV. For this VY interaction, the summations on the intermediate p-h states were carried out to convergence.[16] This truncation difference in the sums for the intermediate p-h states is the largest single difference between the Kuo and VY interactions V_{eff}. Additional but less important differences include the following: (a) Kuo uses plane waves for intermediate particle states while VY use oscillator states; and (b) Kuo places G-matrix vertices on shell while VY keep the off-shell dependence; and (c) Kuo employs an average Pauli operator independent of two-particle center of mass variables while VY have an exact treatment of the Pauli operator.

Since the VY effective interaction was derived from the Reid soft core potential it only includes partial waves for relative total spin values $J \leq 2$. We calculate high spin corrections (HSC) (for $J > 2$) to this interaction directly from two-nucleon scattering phase shifts using the well-known Sussex[7] method. Contributions from a third order diagram were taken from Ref. 8. We mention here that in calculating this third order diagram the intermediate state summations were carried through $6\hbar\Omega$ and were found to be converged owing to large off-shell shifts in certain vertices. For this third order diagram the sign is positive, which means that it should produce a decrease in the calculated binding energy. Except where indicated on the figures, all results labeled V20 ($C = 20$) and V25 ($C = 25$) are calculated with the above mentioned HSC and third order diagram included.

Using the ^{16}O core and slightly adjusted ^{17}O single particle energies $E_{d_{5/2}} = -4.15$, $E_{s_{1/2}} = -3.29$, and $E_{d_{3/2}} = +0.88$ MeV, Chung and Wildenthal developed an empirical interaction for the *sd* shell. Starting with the Kuo matrix elements, these authors compared experimental and calculated shell-model levels for $A = 18$ to $A = 24$ nuclei. About half of the 63 two-body effective interaction matrix elements were adjusted to minimize a χ^2 between the experimental and calculated levels. The quality of the description of the spectra should provide a benchmark for derived effective two-body interactions and we employ the Chung-Wildenthal interaction for this purpose.

The true Hamiltonian $H = T + V$ with kinetic energy operator T depends only on the free nucleon-nucleon interaction V. Ideally, then, H_{eff} should be independent of the chosen single particle Hamiltonian H_0 (and hence independent of $\hbar\Omega$ and C), but when evaluated to fixed order of perturbation theory, some residual dependence is inevitable.

In the case where there is dependence on H_0 it is important to attempt to minimize it. Gambhir and McCarthy[17] examined higher order corrections to Brueckner-Hartree-Fock in ^{16}O and found that when H_0 is chosen such that the low-lying particle spectrum is placed near the "average kinetic" location then these higher order corrections are minimized. That is, for ^{16}O the unoccupied *sd* shell oscillator orbits are placed at +25 MeV, which is the average kinetic energy of a nucleon in this oscillator shell. It is hoped that the higher order diagrams neglected in our V_{eff} will also be

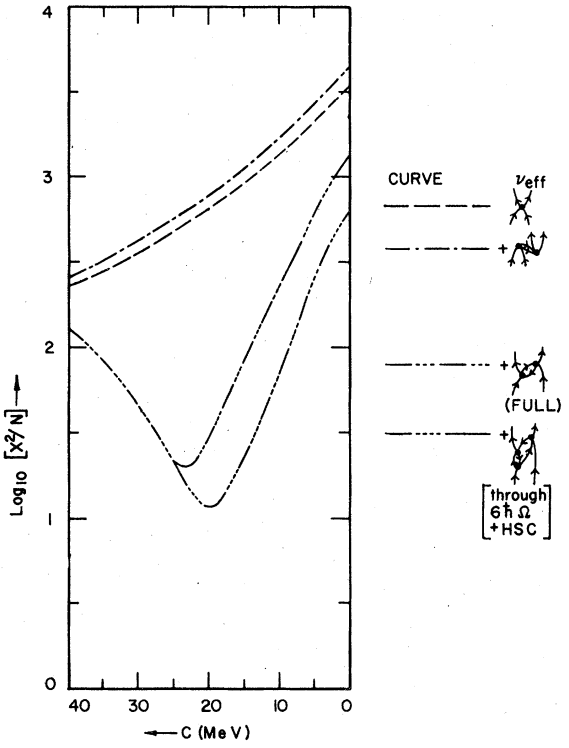

FIG. 2. Logarithm of the χ^2 per degree of freedom N as a function of C for the Vary-Yang interaction with different orders of diagrams and corrections included. The χ^2 is defined with respect to the Chung-Wildenthal (CW) interaction with weights fixed by the error matrix obtained in the CW analysis.

minimized by a corresponding choice where the lowest unoccupied orbits (that is, the *fp* shell for *sd* shell nuclei) are placed at their average kinetic locations. According to Fig. 1, this implies a choice of $C = 20$ MeV when $V_0 = 51.5$ MeV, which is the V_0 we use throughout. This choice of C is within the range of values for which the VY interactions yield, via spectral distribution methods,[10] reasonable binding energies of *sd* shell nuclei.

In Fig. 2 we show a plot of χ^2 vs C (actually $\log_{10}\chi^2/63$) between the VY and CW interactions for different orders of truncation. The χ^2 is defined in terms of linear combinations of matrix elements with a weighting defined by their significance as determined in the CW search procedure.[6] In this way a statistically significant test of the realistic effective interaction may be developed. A brief sketch of the χ^2 test may be found in Ref. 5.

When the core-polarization diagram (with converged intermediate state sums) is included we see in Fig. 2 a minimum for C between 20 and 25 MeV. The addition of an important third order diagram calculated through to convergence by Sandel *et al.*[8] plus some higher partial waves or high spin corrections[7] (HSC) produces a minimum at $C = 20$ MeV. Thus a comparison of the empirical CW interaction with the VY interaction also motivates a choice of C near 20 MeV.

III. MOMENT METHODS AND GLOBAL TEST

In this section we briefly outline the moment expansion techniques for calculating expectation values of operators.[9,11,18] The accuracy of moment expansions for level densities for a given spin J and isobaric spin T (fixed JT) is demonstrated via comparisons against exact diagonalization results. Calculated spin cutoff factors (for ^{28}Si) are compared with experimental values.

To calculate the trace $\langle\langle K\rangle\rangle$ of a scalar operator K for a given spin J we use the well-known formula

$$\langle\langle K\rangle\rangle_{J,M=J} = \langle\langle K\rangle\rangle_{M=J} - \langle\langle K\rangle\rangle_{M=J+1}, \tag{3.1}$$

where M is the projection of the angular momentum on the Z axis.[19] For $K = 1$ this expression gives the number of states of spin J and $M = J$ in terms of the number of states with magnetic projection $M = J$ and $M = J+1$. The level densities for a given isobaric spin $T = T_z$ are calculated from the formula

$$\rho(E,J)_{T,T_z=T} = \rho(E,J)_{T_z=T} - \rho(E,J)_{T_z=T+1}, \tag{3.2}$$

which follows from the isobaric spin space analog of (3.1) for the angular momentum space.

The details we use for calculating the level densities via moment expansions are given in Ref. 11. In Fig. 3 we show $\rho(E,J,T)$ for $J = \frac{9}{2}$ plotted against E for ^{21}Ne ($T = \frac{1}{2}$). This figure demonstrates, as has been done in previous work,[11] that the moment expansion for the level density for fixed J, T is reasonably accurate.

It is also clear from Fig. 3 that most of the average properties of a spectrum for each spin are determined by the energy centroids and widths. For instance, by calculating the widths for two interactions one can infer which interaction will give the more compressed spectrum. In Fig. 4 we show for ^{21}Ne calculated energy centroids and widths versus twice the spin for the Kuo, CW, V25, and V20 interactions. We also show the values (black dots) for these moments calculated with the shell-model code using the CW interaction. By comparing the two CW calculations we can see that the above expansions for the centroid and widths as a function of J are reasonably accurate except for large J, where the dimensions are so small ($\lesssim$1 level/MeV) that the moment expansions are not very meaningful.

Several features of the results shown in Fig. 4 are noteworthy. First, the fact that the V20 and

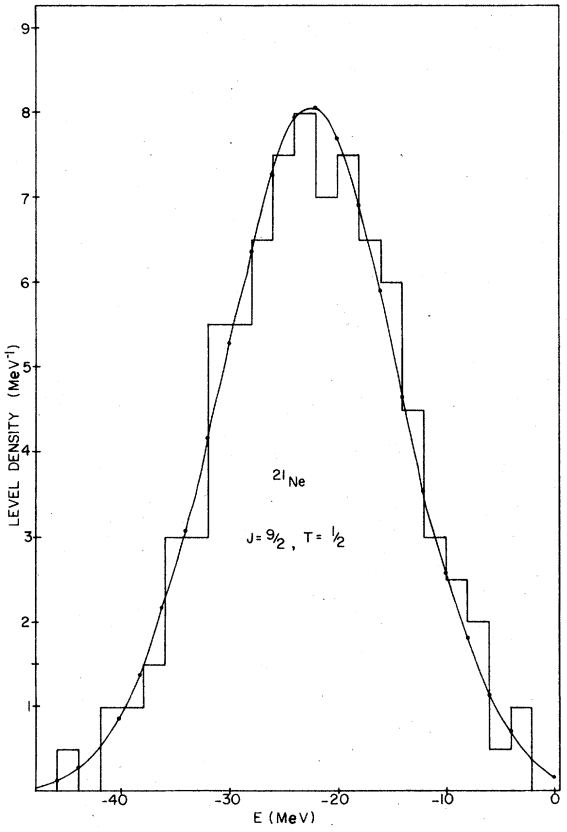

FIG. 3. Fixed-JT-level density vs energy. The smooth curve is determined by summing the configuration contributions calculated with spectral distribution theory. The histogram depicts the level density obtained from exact shell-model diagonalization with the same interaction (CW).

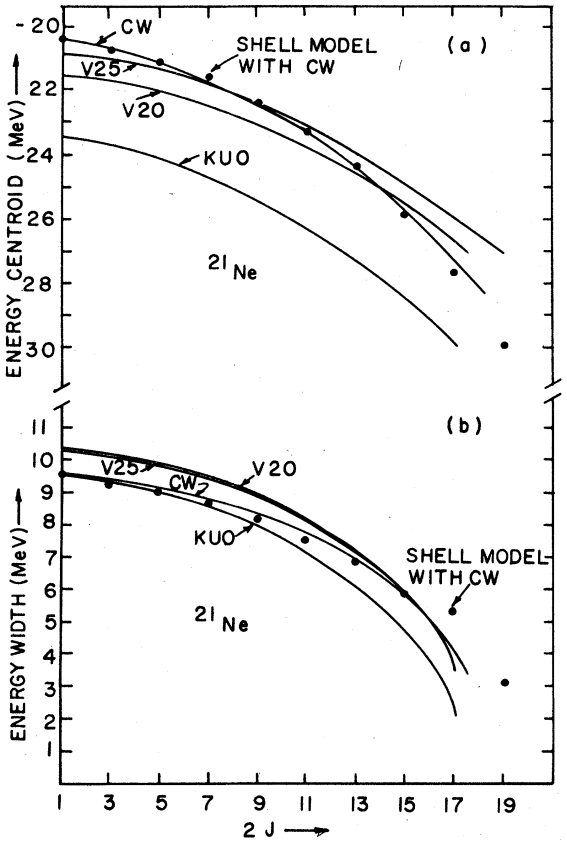

FIG. 4. (a) ^{21}Ne energy centroids vs twice the spin for the CW, Kuo, V25, and V20 interactions. (b) ^{21}Ne energy widths versus twice the spin for the CW, Kuo, V25, and V20 interactions. The shell-model values calculated with the CW interaction are indicated with dots.

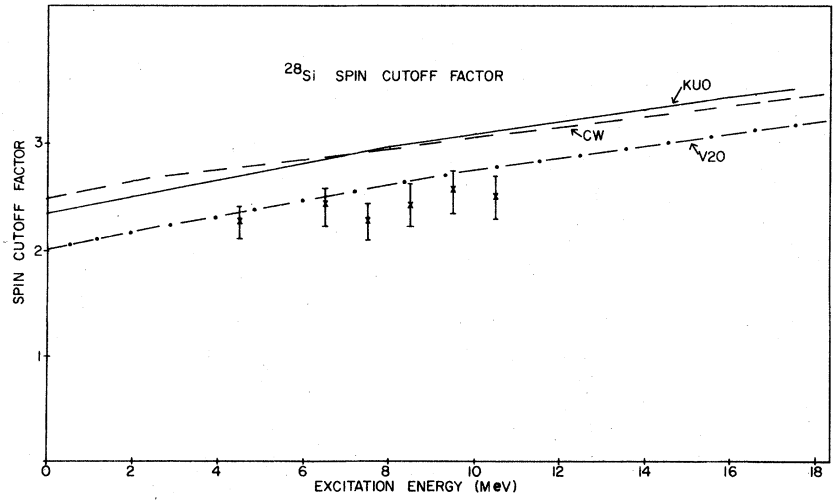

FIG. 5. Spin cutoff factor vs energy. The experimental values with error bars shown were obtained from Ref. 11. The calculated values for three different interactions are shown.

V25 Hamiltonians yield less attractive centroids than the Kuo Hamiltonian is a reflection of the fact that the more accurate treatment of core polarization by Vary and Yang reduces the attractiveness of the diagonal two-particle matrix elements. Second, the larger width of V20 and V25 over the Kuo interaction reflects the fact that a more accurate treatment of core polarization increases the magnitude of off-diagonal two-particle matrix elements. Both these features were indicated in earlier studies[16] but are confirmed here for all J values and for multiparticle spectra. Finally, from the values shown in Fig. 4(b) we would expect that for all except the largest spin values, the CW and Kuo interactions would give a more compressed spectrum than would be obtained from the V20 and V25 interactions. In the next section we shall show that this feature is indeed reflected in the exact shell-model spectra. The point of interest here is that comparisons of average spectral properties for different interactions can be obtained through their moments. Furthermore, these moments are readily calculated for systems where shell-model diagonalizations are not feasible.

Of particular interest in studies of compound nuclear reaction cross sections[20] in the statistical region is the spin cutoff factor $\lambda(E)$. This quantity arises in approximating the difference in (3.1) for $K=1$ by a derivative at $M=J+\frac{1}{2}$. This gives the following approximate formula for the spin dependence of the level density:

$$\rho_{J,M=J} \propto (2J+1)\exp[-J(J+1)/2\lambda^2(E)]. \qquad (3.3)$$

Here, $\lambda^2(E)=\langle J_z^2\delta(H-E)\rangle$ is the average expectation value of J_z^2 at a given energy E.

In Fig. 5 we show the calculated values of $\lambda(E)$ for ^{28}Si for the three different interactions mentioned earlier. The calculated curves shown for $\lambda(E)$ are approximate in that they were calculated only through the $P_2(H)$ term defined in Ref. 11. Shown also in this plot are some experimental values for $\lambda(E)$ obtained from fitting angular distributions in a recently measured ^{25}Mg$(\alpha,n)^{28}$Si reaction.[11]

The curves for $\lambda(E)$ in Fig. 5 each have approximately the same slope as the experimental data. Calculations with up-to-date thermodynamic models produce larger slopes for $\lambda(E)$, a feature thought to be due to the noninclusion of two-body interactions in these models.[20] It is worthwhile to notice that $\lambda(E)$ calculated with the CW and Kuo interactions are very close. This could be due to a lingering correlation resulting from the use of the Kuo matrix elements as initial values in the search procedure for the CW matrix elements.

As we mentioned above, the curves in Fig. 5 were calculated through the $P_2(H)$ term defined in Ref. 11. Truncation at the P_1 term (not shown) gives values for $\lambda(E)$ about 0.45 above the values shown with approximately the same slope. These first order results are consistent with those calculated by Wong and Lougheed,[21] who truncated at the P_1 term. However, the large difference between the P_1 and P_2 truncations indicates that inclusion of higher order terms may be needed before sufficient convergence is obtained.

IV. SHELL-MODEL SPECTRA

In this section we compare shell-model spectra for several $A=18$–21 nuclei calculated with the Kuo, VY, and CW interactions. We also discuss the effects of adding to the interaction some high spin corrections (HSC) and contributions from one major third order diagram. In each case we as-

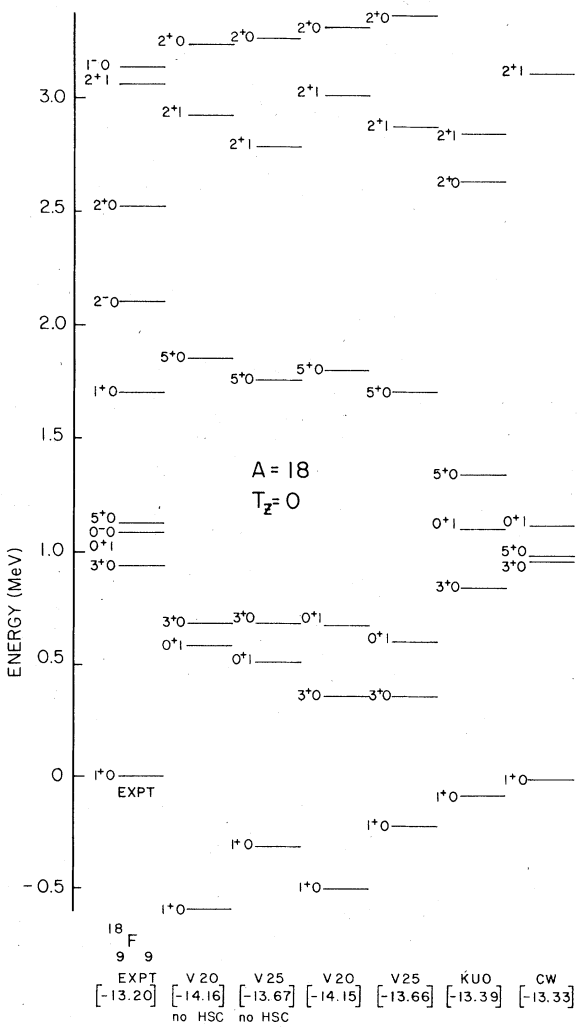

FIG. 6. Spectra for mass 18, $T=0$.

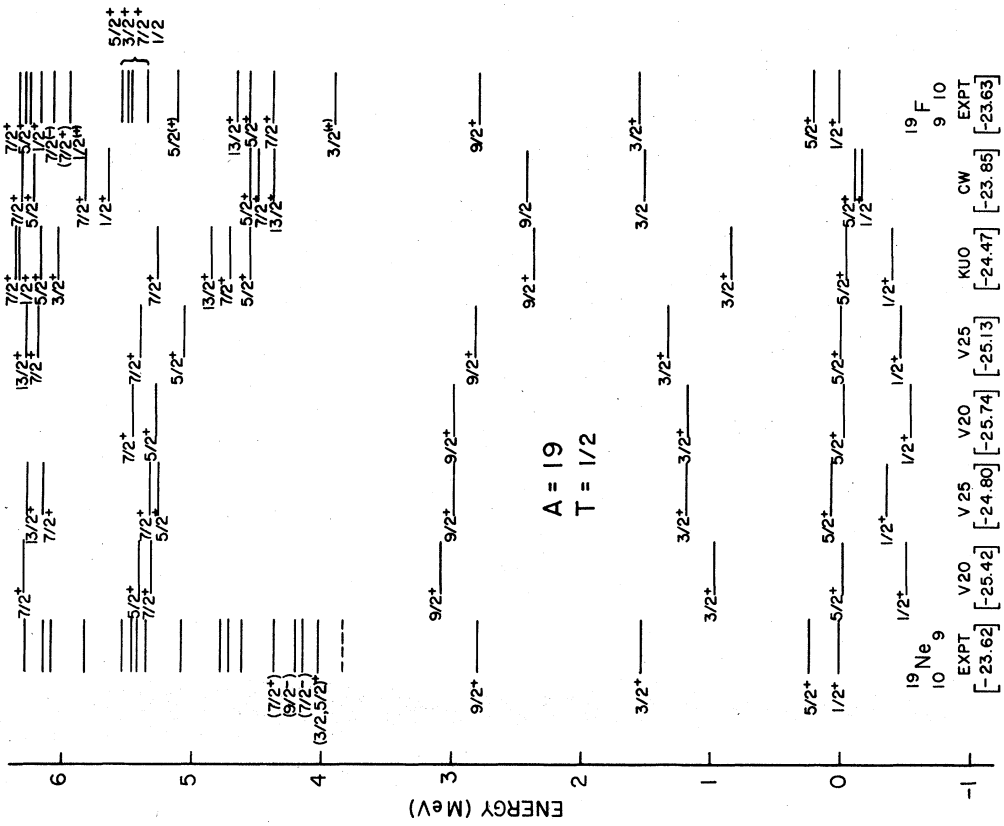

FIG. 8. Spectra for mass 19, $T=\frac{1}{2}$.

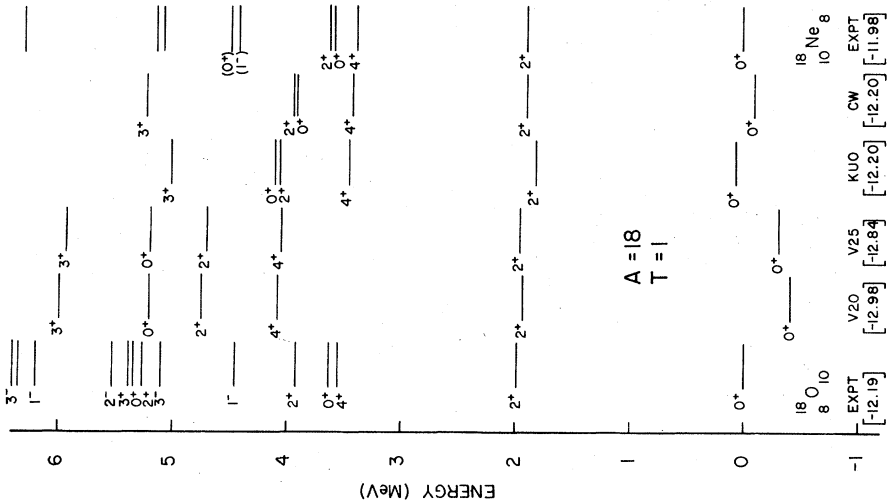

FIG. 7. Spectra for mass 18, $T=1$.

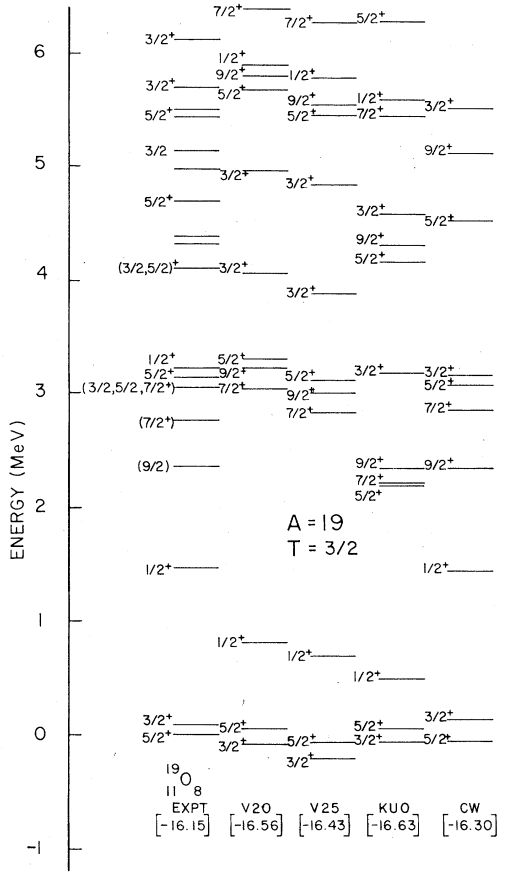

FIG. 9. Spectra for mass 19, $T=\frac{3}{2}$.

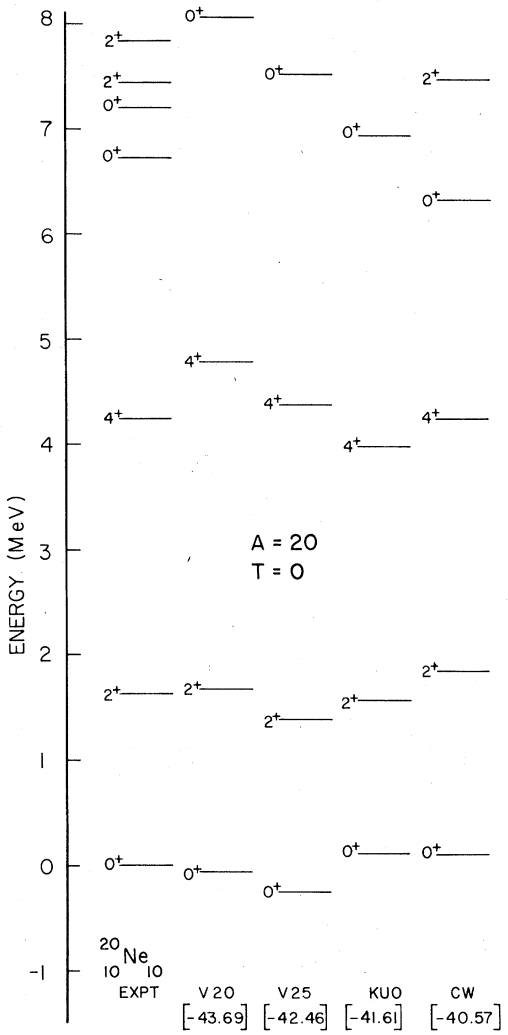

FIG. 10. Spectra for mass 20, $T=0$.

sumed an ^{16}O core and experimental single-particle energies. The calculations were made with the Rochester–Oak Ridge Shell Model Code.[12]

The calculated spectra are shown in Figs. 6–12. The experimental values shown in Figs. 6–10 were taken from Ref. 22 and those shown in Figs. 11 and 12 were taken from Ref. 23. The spectrum in each case was shifted relative to the experimental spectrum using a least squares fit. The calculated ground-state binding energies relative to ^{16}O are shown on the figures in each case.

In Figs. 11 and 12 we show the spectrum of ^{21}Ne calculated using the VY interaction with and without the third order diagram included. Comparing these spectra, we see that the third order diagram has at least two noticeable effects. One effect is to decrease the calculated binding energy for ^{21}Ne relative to ^{16}O by about 1 MeV. A decrease was expected from the positive nature of the diagram. This particular effect is in the direction needed for the calculated spectra to agree better with the data. A second effect is to produce some additional splitting of levels, most noticeably for the $\frac{7}{2}^+$ and $\frac{1}{2}^+$ second and third excited states. This additional splitting also improves the agreement between the calculated and experimental spectra. In general, the addition of this third order diagram tends to improve the overall agreement between the experimental and calculated spectra. We note here, however, that we have included only this third order diagram because none of the remaining diagrams have been calculated with converged intermediate state sums. By including it we do not wish to imply that it is the major contribution of third order. A full third order calculation of the same precision as that of the work of Sandel *et al.*[8] would be desirable to complete our current picture of convergence.

In Figs. 6, 8, and 11 we show spectra calculated with and without the HSC effects. The HSC effects on the spectra for Figs. 7, 9, and 10 were too small to warrant plotting both spectra separately. The HSC appears to produce compression of levels

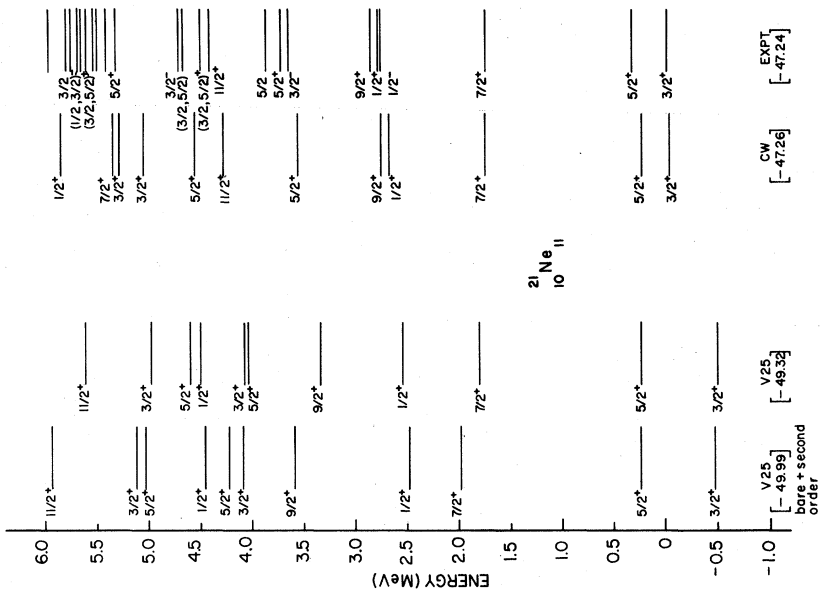

FIG. 12. Spectra for mass 21, $T=\frac{1}{2}$.

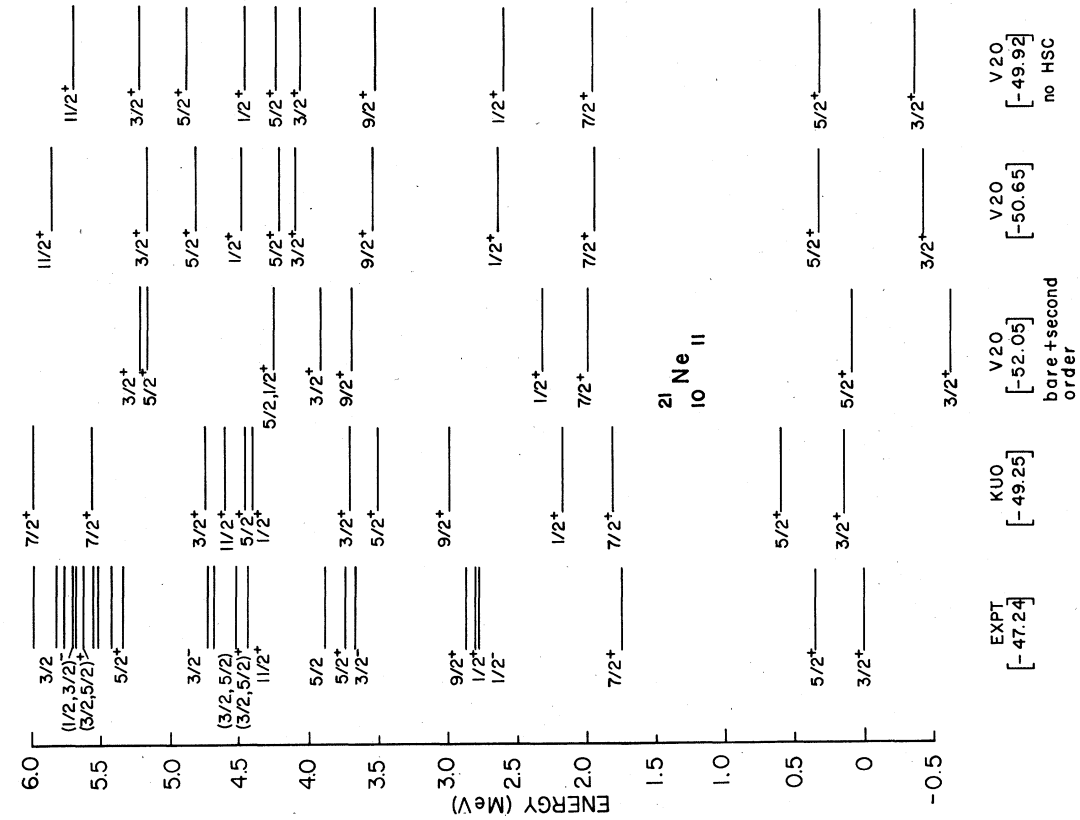

FIG. 11. Spectra for mass 21, $T=\frac{1}{2}$.

in some cases and spreading in others, but the size of the effects are generally small. The compression is most appreciable for the lowest level splitting for $A = 18$ ($T = 0$) shown in Fig. 6.

For most of the calculated spectra the CW interaction gives, as expected, the best agreement with the experimental spectra. The Kuo interaction produces the next best agreement. The VY interactions, either with or without the above mentioned corrections, produce the poorest agreement with the data.

The difference between the spectra calculated with the VY ($C = 20$) and with the VY ($C = 25$) interactions can be seen from the figures. The $C = 25$ interaction generally produces a slightly more compressed spectrum. This result is consistent with the results in Fig. 4, where we show that the width for the V25 interaction is slightly smaller than the width for the V20 interaction. More binding is obtained for the $C = 20$ interaction. This result is likewise consistent with Fig. 4(a), which shows that the energy centroid for the V20 interaction is about 1 MeV below the energy centroid for the V25 interaction.

ACKNOWLEDGMENTS

The authors would like to thank Dr. M. Sandel for reading this manuscript and Dr. S. Grimes for providing the spin cutoff data and for useful discussions. Dr. B. H. Wildenthal and Dr. W. Chung are acknowledged for useful conversations and providing us with their interaction and related information. This work was supported by the U. S. Department of Energy, Contract No. W-7405-Eng-82, Office of Basic Sciences, Nuclear Physics Division.

---

*Present address: Dept. of Science and Mathematics, Park's College, Cahokia, Illinois 62206.

[1]K. A. Brueckner, Phys. Rev. 97, 1353 (1955).
[2]Effective Interactions and Operators in Nuclei, edited by B. R. Barrett (Springer, Berlin, 1975).
[3]P. J Ellis and E. Osnes, Rev. Mod. Phys. 49, 777 (1977).
[4]T. T. S. Kuo, Nucl. Phys. A103, 71 (1967).
[5]J. P. Vary and S. N. Yang, Phys. Rev. C 15, 1545 (1977).
[6]W. Chung and B. H. Wildenthal (private communication); W. Chung, Ph.D. thesis (Michigan State University, 1976) (unpublished); B. H. Wildenthal, Nukleonika 23, 549 (1978), and references quoted therein.
[7]J. P. Elliott, A. D. Jackson, H. A. Mavromatis, E. A. Sanderson, and B. Singh, Nucl. Phys. A121, 241 (1968); A. W. Gregersen and S. A. Williams (unpublished).
[8]M. S. Sandel, R. J. McCarthy, B. R. Barrett, and J. P. Vary, Phys. Rev. C 17, 777 (1978).
[9]See for instance F. S. Chang, J. B. French, and T. H. Thio, Ann. Phys. (N. Y.) 66, 137 (1971); J. B. French, Rev. Mex. Fis. 23, 189 (1974); K. F. Ratcliff, Phys. Rev. C 3, 117 (1971); J. P. Draayer, J. B. French, and S. S. M. Wong, Ann. Phys. (N. Y.) 196, 472 (1977).
[10]B. J. Dalton, J. P. Vary and W. J. Baldridge, Phys. Rev. Lett. 38, 1348 (1977).
[11]See for instance S. M. Grimes, C. H. Poppe, C. Wong, and B. J. Dalton, Phys. Rev. C 18, 1100 (1978).
[12]J. B. French, E. C. Halbert, J. B. McGrory, and S. S. M. Wong, in Advances in Nuclear Physics, edited by M. Baranger and E. Vogt (Plenum, New York, 1969), Vol. 3, p. 193.
[13]C. Bloch and J. Horowitz, Nucl. Phys. 8, 91 (1958); B. H. Brandow, Rev. Mod. Phys. 39, 771 (1967).
[14]T. Hamada and I. D. Johnston, Nucl. Phys. 34, 382 (1962).
[15]R. V. Reid, Ann. Phys. (N. Y.) 50, 411 (1968).
[16]The large effects due to truncation of intermediate state sums in V_{eff} are discussed at length in J. P. Vary, P. U. Sauer, and C. W. Wong, Phys. Rev. C 7, 1976 (1973).
[17]One can successfully minimize the effects of certain higher order diagrams in BHF calculations [see Y. K. Gambhir and R. J. McCarthy, Nucl. Phys. A228, 246 (1974)] with a shifted oscillator that puts lowest unoccupied states at their average kinetic energy.
[18]J. N. Ginocchio, Phys. Rev. C 8, 135 (1973); S. Ayik and J. N. Ginocchio, Nucl. Phys. A221, 285 (1974); A234, 13 (1974); see also C. Quesne, J. Math. Phys. 16, 2427 (1975); B. D. Chang and S. S. M. Wong, Nucl. Phys. A294, 19 (1978).
[19]The first expansions for the angular momentum projection dependence of moments [J. N. Ginocchio and M. M. Yen, Nucl. Phys. A239, 365 (1975)] were obtained using linear response theory. The expansion in (3.1) follows Ref. 11 in using a characteristic polynominal expansion.
[20]S. M. Grimes, J. D. Anderson, J. W. McClure, B. A. Pohl, and C. Wong, Phys. Rev. C 10, 2372 (1974). See Ref. 11 also.
[21]S. S. M. Wong and G. D. Lougheed, Nucl. Phys. A295, 289 (1978).
[22]F. Ajzenberg-Selove, Nucl. Phys. A190, 1 (1972).
[23]P. M. Endt and C. Van Der Leun, Nucl. Phys. A214, 1 (1973).